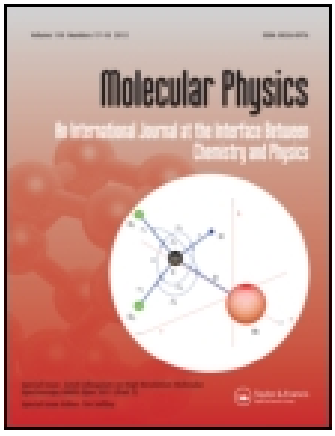

Molecular Physics: An International Journal at the Interface Between Chemistry and Physics
Publication details, including instructions for authors and subscription information:
http://www.tandfonline.com/loi/tmph20

The infrared spectrum of $^{13}C_2H_2$ in the 60-2600 cm^{-1} region: bending states up to $v_4+v_5=4$

Adriana Predoi-Cross [a], Michel Herman [b], Luciano Fusina [c] & Gianfranco Di Lonardo [c]

[a] Alberta Terrestrial Imaging Centre, Department of Physics and Astronomy, University of Lethbridge, 4401 University Drive, Lethbridge AB, T1K 3M4, Canada

[b] Laboratoire de Chimie Quantique et Photophysique, CP 160/09, Faculté des Sciences, Université Libre de Bruxelles, 50 Av., Roosevelt, B-1050 Bruxelles, Belgium

[c] Dipartimento di Chimica Fisica e Inorganica, Facoltà di Chimica, Industriale, Università di Bologna, Viale Risorgimento 4, 40136, Bologna, Italy

Accepted author version posted online: 25 Jun 2012.Published online: 18 Jul 2012.

To cite this article: Adriana Predoi-Cross, Michel Herman, Luciano Fusina & Gianfranco Di Lonardo (2012) The infrared spectrum of $^{13}C_2H_2$ in the 60-2600 cm^{-1} region: bending states up to $v_4+v_5=4$, Molecular Physics: An International Journal at the Interface Between Chemistry and Physics, 110:21-22, 2621-2632, DOI: 10.1080/00268976.2012.705345

To link to this article: http://dx.doi.org/10.1080/00268976.2012.705345

Molecular Physics
Vol. 110, Nos. 21–22, November 2012, 2621–2632

Taylor & Francis
Taylor & Francis Group

SPECIAL ISSUE: FASE (FEMTO-, ASTRO-, SPECTRO-ETHYNE)

The infrared spectrum of $^{13}C_2H_2$ in the 60–2600 cm^{-1} region: bending states up to $v_4 + v_5 = 4$

Adriana Predoi-Cross[a], Michel Herman[b], Luciano Fusina[c] and Gianfranco Di Lonardo[c]*

[a]*Alberta Terrestrial Imaging Centre, Department of Physics and Astronomy, University of Lethbridge, 4401 University Drive, Lethbridge AB, T1K 3M4, Canada;* [b]*Laboratoire de Chimie Quantique et Photophysique, CP 160/09, Faculté des Sciences, Université Libre de Bruxelles, 50 Av., Roosevelt, B-1050 Bruxelles, Belgium;* [c]*Dipartimento di Chimica Fisica e Inorganica, Facoltà di Chimica, Industriale, Università di Bologna, Viale Risorgimento 4, 40136, Bologna, Italy*

(*Received 14 May 2012; final version received 15 June 2012*)

The vibration–rotation spectra of ^{13}C substituted acetylene, $^{13}C_2H_2$, have been recorded in the region between 60 and 2600 cm^{-1} at an effective resolution ranging from 0.001 to 0.006 cm^{-1}. Three different instruments were used to collect the experimental data in the extended spectral interval investigated. In total 9529 rotation vibration transitions have been assigned to 101 bands involving the bending states up to $v_{tot} = v_4 + v_5 = 4$, allowing the characterization of the ground state and of 33 vibrationally excited states. All the bands involving states up to $v_{tot} = 3$ have been analyzed simultaneously by adopting a model Hamiltonian which takes into account the vibration and rotation *l*-type resonances. The derived spectroscopic parameters reproduce the transition wavenumbers with a RMS value of the order of the experimental uncertainty. Using the same model, larger discrepancies between observed and calculated values have been obtained for transitions involving states with $v_{tot} = 4$. These could be satisfactorily reproduced only by adopting a set of effective constants for each vibrational manifold, in addition to the previously determined parameters, which were constrained in the analysis.

Keywords: $^{13}C_2H_2$; high-resolution Fourier transform infrared spectroscopy; fundamental; combination; overtone; hot bands; global analysis

1. Introduction

Apart from early pioneering works [1–5], during the last 20 years the infrared spectrum of $^{13}C_2H_2$ has been the subject of several investigations [6–13]. In 1993 Di Lonardo *et al.* [6] reported on the bending states of this molecule up to $v_4 + v_5 = 2$. In the region between 50 and 1450 cm^{-1} 1203 transitions were assigned to 20 bands, characterizing, in addition to the ground state, eight different bending states. The anharmonic interactions in the $v_1/v_2 + 2v_5$ dyad were studied and the interaction constants were characterized together with the excited state molecular parameters [7]. The quartic anharmonic resonances for the combination levels $v_1 + mv_4 + nv_5$, $v_2 + mv_4 + (n+2)v_5$ and $v_3 + (m-1)v_4 + (n+1)v_5$ were investigated in the region 2000–5200 cm^{-1} [8]. The stretching fundamentals were further studied and the perturbed and deperturbed G_v^0 values for the $v_1 = 1$, $v_2 = 1$ and $v_3 = 1$ states were reported [9]. The Raman spectrum of this molecule was recorded both at medium resolution [10] up to 5300 cm^{-1} and at high resolution [11,12] up to 4000 cm^{-1} giving a direct access to the states manifolds of *g* symmetry. Molecular parameters of many vibrational states not accessible by conventional electric dipole selection rules were evaluated. In 1999 a total of 134 vibrational levels in the electronic ground state were gathered for this molecule and fitted to 29 vibrational constants [13]. The tentative assignment of $4\nu_4$ Σ_g^+ at 2448.74 cm^{-1} was not confirmed in the present work.

In this study we have extended up to $v_{tot} = 4$ the previous observations of the bending states by means of spectra recorded at higher resolution and dynamical detection range, covering a larger spectral region by means of different experimental setups. Some results (G_v^0 and B_v) obtained from "band-by-band" analysis for several excited bending states have been already reported [13]. The experiments are described in Section 2. The description of the spectra and the assignments are presented in Section 3, and the band-by-band and global analyses in Section 4, together with the discussion of the results.

2. Experimental details

The spectra were recorded using three different instruments. In the region between 60 and 300 cm^{-1} a single absorption spectrum was recorded at a pressure of

*Corresponding author. Email: gianfranco.dilonardo@unibo.it

ISSN 0026–8976 print/ISSN 1362–3028 online

http://dx.doi.org/10.1080/00268976.2012.705345
http://www.tandfonline.com

362 Pa and 72 m optical path, using the Bruker IFS 125 Fourier transform spectrometer located at the far-infrared beamline, Canadian Light Source, Canada. On the same apparatus two spectra were recorded in the region 400–600 cm^{-1} at pressures of 18.7 and 360.0 Pa and 72 m optical path. Optimum instrumental performance was achieved using the synchrotron source, 6 μm Mylar beamsplitter and Si bolometer detector cooled at 4 K. The spectrometer aperture was set to 1.7 mm. A scanner velocity of 80 kHz was used with a 5 kHz analog electronic low band pass filter. No optical filter was used. The boxcar apodization adopted during the Fourier transform process led to an instrumental full width at half maximum of 0.00096 cm^{-1} (0.61/optical path length difference). A zero-filling factor of 2, Mertz phase correction, and phase resolution of 1.0 were also used to process the spectra. All the spectra were recorded using a multipass coolable absorption cell of 2 m base, with wedged polypropylene windows, set for 72 m path length. The sample was supplied by Sigma-Aldrich with a purity of 98% and used without any further purification. All the spectra were recorded at 298 K.

In the region 400–600 cm^{-1} we have recorded two spectra at 19.4 Pa and 362 Pa. All the resources were identical to the previous recording with the exception of the Ge:Cu detector and an aperture of 1.15 mm. The gas pressure was measured using a 0–1 torr Baratron gauge for the spectrum recorded at 19.4 Pa, and a 0–10 torr one for the spectrum at 362 Pa.

Since all the bands have been fitted simultaneously, particular care was devoted to the calibration of these spectra and of those described below. Rotational water lines [14–16] were used to calibrate the wavenumber scale, but no correction was applied since the calculated deviation was much smaller than the accuracy of the measurements.

The spectra in the region between 600 and 850 cm^{-1} were recorded at NRCC in Ottawa by means of a modified Bomem DA3.002 FT spectrometer. Three spectra were recorded at different pressures (0.27 Pa, 33.33 Pa and 73.32 Pa) and path length of 4 m at a resolution of 0.002 cm^{-1}, while a fourth one was recorded in the region 420–756 cm^{-1} at a resolution of 0.003 cm^{-1}, optical path length of 72 m and pressure of 93.32 Pa. The spectra were calibrated by means of pure rotational water lines [14, 16] and of transitions in the ν_1 band of OCS added in the cell [17–18].

All the spectra in the region between 1000 and 2800 cm^{-1} were recorded at University of Bologna on a Bomem DA3 002 at a resolution of 0.004 or 0.006 cm^{-1}, path length ranging from 2 to 10 m, and pressure in the range 133–1333 Pa. Calibration of wavenumbers was achieved by means of lines of the ν_1, ν_2 and ν_3 bands of water [19] and of the ν_3 band of CO_2 [20], corrected as suggested by Guelachvili *et al.* [21].

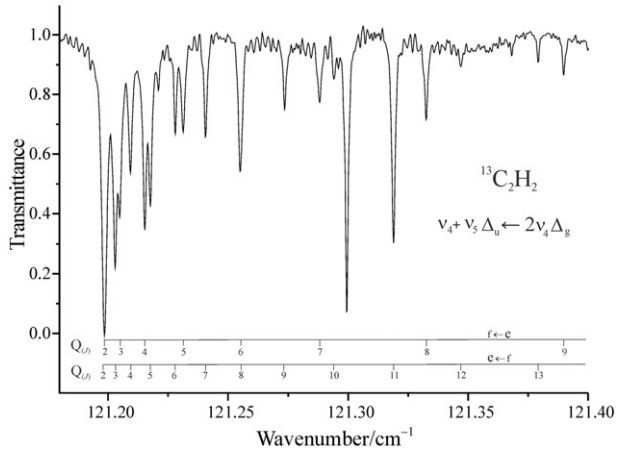

Figure 1. Portion of the infrared spectrum of $^{13}C_2H_2$ in the FIR region showing the Q-branch transitions of the $(\nu_4+\nu_5)$, $\Delta_u \leftarrow 2\nu_4$, Δ_g band. Experimental conditions: pressure, 364 Pa; path length, 72.0 m; resolution, 0.00096 cm^{-1}.

3. Description of the spectra

3.1. *The far infrared region*

The spectrum in the far infrared (FIR) region (60–250 cm^{-1}) is very similar to that of $^{12}C_2H_2$ [22], only shifted towards higher wavenumbers by about 7 cm^{-1}. A total of 18 bands concerning states with ν_{tot} up to 3 were observed. The spectrum is dominated by the $P(J)$ and $R(J)$ branches of the ν_5, $\Pi u \leftarrow \nu_4$, Πg transition and associated hot bands. Figure 1 shows one of the four Q branches observed in this region of the spectrum, namely that of $(\nu_4+\nu_5)$, $\Delta u \leftarrow 2\nu_4$, Δg. Four perturbation allowed bands were also detected because of the mixing of the (e) levels due to the l-type resonance.

3.2. *The 400–850 cm^{-1} region*

In the lower part of the spectrum (400–600 cm^{-1}) a particular set of hot bands can be seen, having the $2\nu_4$, $3\nu_4$ and $2\nu_4+\nu_5$ manifolds as upper states. Owing to the weak nature of these bands no trace of the $4\nu_4$ manifold has been detected. Figure 2 shows the $Q(J)$ branch of the $3\nu_4$, $\Pi_g \leftarrow (\nu_4+\nu_5)$, Σ_u^-. The upper part of the spectrum is dominated by the very strong ν_5, $\Pi_u \leftarrow GS$, Σ_g^+ centred at 727.23 cm^{-1} and associated hot bands involving states up to $\nu_{tot}=4$. As an example, the $(2\nu_4+2\nu_5)$, $\Sigma_g^- \leftarrow (2\nu_4+\nu_5)$, $^{II}\Pi_u$ is

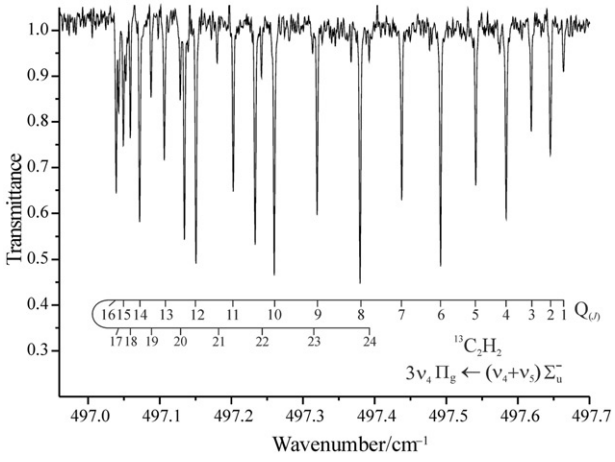

Figure 2. Portion of the infrared spectrum of $^{13}C_2H_2$ in the 500 cm^{-1} region showing the Q-branch transitions of the $3\nu_4$, $\Pi_g \leftarrow (\nu_4+\nu_5)$, Σ_u^- band. Experimental conditions: pressure, 364 Pa; path length, 72.0 m; resolution, 0.002 cm^{-1}.

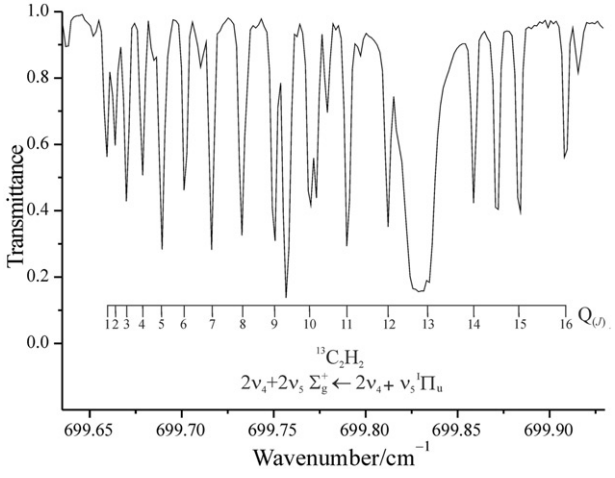

Figure 3. Portion of the infrared spectrum of $^{13}C_2H_2$ in the 700 cm^{-1} region showing the Q-branch transitions of the $(2\nu_4+2\nu_5)$, $\Sigma_g^+ \leftarrow (2\nu_4+\nu_5)$, $^1\Pi_u$ band. Experimental conditions: pressure, 93.32 Pa; path length, 72.0 m; resolution, 0.003 cm^{-1}.

shown in Figure 3. In particular, thanks to excellent resolution and sensitivity of the spectrum recorded with 72 m optical path length, we observed the $4\nu_5$, $\Gamma g \leftarrow 3\nu_5$, Φ_u band involving states with very high vibrational angular momentum.

3.3. *The 1200–1450 cm^{-1} region*

This region is dominated by the strong $(\nu_4+\nu_5)$, $\Sigma_u^+ \leftarrow$ GS, Σ_g^+ and associated hot bands. In total 13

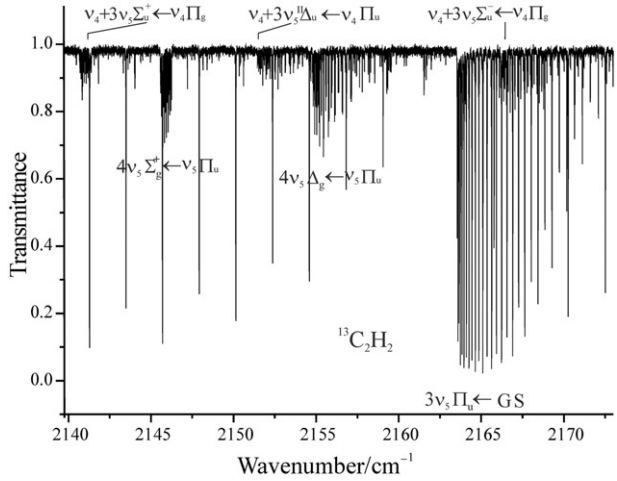

Figure 4. Portion of the infrared spectrum of $^{13}C_2H_2$ in the 2150 cm^{-1} region showing the Q-branch transitions of the $3\nu_5$, $\Pi_u \leftarrow$ GS, Σ_g^+ and associated hot bands. Experimental conditions: pressure, 1333 Pa; path length, 10.0 m; resolution, 0.006 cm^{-1}.

vibration–rotation bands have been identified and analyzed, 12 characterized by the $\Delta l = 0$ selection rule. One band, with origin at 1332.16 cm^{-1}, is perturbation allowed ($\Delta l = \pm 2$) of the kind $\Delta_u\,(e) \leftarrow \Sigma_g^+(e)$.

3.4. *The 1800–2200 cm^{-1} region*

In this spectral range 15 vibration–rotation bands have been identified. Three of them originate from the ground state, namely the $2\nu_4+\nu_5$, $^I\Pi_u$ and $^{II}\Pi_u$ and the $3\nu_5$, Π_u. Figure 4 illustrates an overall view of the region 2140–2170 cm^{-1} containing the $3\nu_5 \leftarrow$ GS and associated hot bands.

3.5. *The 2300–2700 cm^{-1} region*

In this region only two bands are detected, namely $(3\nu_4+\nu_5)$, $\Sigma_u^+ \leftarrow$ GS, Σ_g^+ and the perturbation allowed $(3\nu_4+\nu_5)$, $^{II}\Delta_u \leftarrow$ GS, Σ_g^+. The latter is relatively strong because the (e) levels of the $^{II}\Delta_u$ state are very close to those of the Σ_u^+ state of the same manifold.

In addition, the $\nu_2 \leftarrow \nu_5$, $\nu_1 \leftarrow \nu_5$ and $\nu_3 \leftarrow \nu_4$ difference bands and the $\nu_2+\nu_5 \leftarrow$ GS stretching–bending combination band are also observed in various regions of the spectrum. The analysis of all these bands, together with additional stretching–bending combination bands observed at higher wavenumbers, has been reported elsewhere [6–13].

The recorded lines were assigned on the basis of the previously reported data for the same molecule and of the corresponding spectra of the symmetric and asymmetric isotopologues, $^{12}C_2H_2$ [25] and $^{13}C^{12}CH_2$

[26]. Lower state combination differences were used to assign the J values of the transitions and also to identify the lower energy vibrational state. This identification helped the vibrational assignment of the bands, which was also accomplished by comparison with those of the $^{12}C_2H_2$ [25] and $^{13}C^{12}CH_2$ [26].

4. Analysis

Table 1 lists the analyzed bands together with the symmetry of the vibrational states involved in the transitions, the band centre, the observed range of J values for the various sub-bands, and the RMS error resulting from the simultaneous least-squares analysis described below. The band centre is defined as

$$\nu_C = G^0_{\upsilon'} - B_{\upsilon'}k^2 - D_{\upsilon'}k^4 - (G^0_{\upsilon''} - B_{\upsilon''}k^2 - D_{\upsilon''}k^4) \quad (1)$$

where $G^0_{\upsilon'}$ and $G^0_{\upsilon''}$ represent the purely vibrational energy of the upper and lower state and the quantum number $k=(l_4+l_5)$ is the total vibrational angular momentum.

In the first stages of the analysis, band-by-band fits were performed in order to verify the assignments and to predict the position of very weak lines in congested regions of the spectra. In this way we have also extended the J range of the transitions of the previously observed bands [6,13]. After having identified all the transitions involving pure bending states we performed a simultaneous fit.

The model Hamiltonian adopted for the analysis is analogous to that used for the study of the bending states in $^{12}C_2H_2$ [23] and $^{13}C_2H_2$ [6]. It is based on an extension up to four quanta of excitation, $\nu_{tot}=4$, of the Hamiltonian for a molecule with two bending vibrations [24]. The energies of the rotation–vibration levels of the transitions were obtained by diagonalizing the appropriate energy matrix containing the following vibration (G^0) and rotation (F) diagonal contributions:

$$\begin{aligned}
&G^0(v_4,l_4,v_5,l_5)\\
&= \omega^0_4 v_4 + \omega^0_5 v_5 + x^0_{44}(v_4)^2\\
&\quad + x^0_{45}v_4v_5 + x^0_{55}(v_5)^2 + g^0_{44}(l_4)^2 + g^0_{45}l_4l_5 + g^0_{55}(l_5)^2\\
&\quad + y^0_{444}(v_4)^3 + y^0_{445}(v_4)^2v_5 + y^0_{455}v_4(v_5)^2 + y^0_{555}(v_5)^3\\
&\quad + y^{44}_4 v_4(l_4)^2 + y^{45}_4 v_4l_4l_5 + y^{55}_4 v_4(l_5)^2 + y^{44}_5 v_5(l_4)^2\\
&\quad + y^{45}_5 v_5l_4l_5 + y^{55}_5 v_5(l_5)^2 + y^0_{4444}(v_4)^4 + y^0_{4445}(v_4)^3v_5\\
&\quad + y^0_{4455}(v_4)^2(v_5)^2 + y^0_{4555}v_4(v_5)^3 + y^0_{5555}(v_5)^4\\
&\quad + y^{44}_{44}(v_4)^2(l_4)^2 + y^{45}_{44}(v_4)^2l_4l_5 + y^{55}_{44}(v_4)^2(l_5)^2\\
&\quad + y^{44}_{45}v_4v_5(l_4)^2 + y^{45}_{45}v_4v_5l_4l_5 + y^{55}_{45}v_4v_5(l_5)^2\\
&\quad + y^{44}_{55}(v_5)^2(l_4)^2 + y^{45}_{55}(v_5)^2l_4l_5 + y^{55}_{55}(v_5)^2(l_5)^2 \qquad (2)
\end{aligned}$$

$$\begin{aligned}
&F(v_4,l_4,v_5,l_5)\\
&= [B_0 - \alpha_4v_4 - \alpha_5v_5 + \gamma_{44}(v_4)^2 + \gamma_{45}v_4v_5 + \gamma_{55}(v_5)^2\\
&\quad + \gamma^{44}(l_4)^2 + \gamma^{45}l_4l_5 + \gamma^{55}(l_5)^2 + \gamma_{444}(v_4)^3\\
&\quad + \gamma_{445}(v_4)^2v_5 + \gamma_{455}v_4(v_5)^2 + \gamma_{555}(v_5)^3\\
&\quad + \gamma^{44}_4 v_4(l_4)^2 + \gamma^{45}_4 v_4l_4l_5 + \gamma^{55}_4 v_4(l_5)^2\\
&\quad + \gamma^{44}_5 v_5(l_4)^2 + \gamma^{45}_5 v_5l_4l_5 + \gamma^{55}_5 v_5(l_5)^2\\
&\quad + \gamma_{4444}(v_4)^4 + \gamma_{4445}(v_4)^3(v_5) + \gamma_{4455}(v_4)^2(v_5)^2\\
&\quad + \gamma_{4555}(v_4)(v_5)^3 + \gamma_{5555}(v_5)^4 + \gamma^{44}_{44}(v_4)^2(l_4)^2\\
&\quad + \gamma^{45}_{44}(v_4)^2l_4l_5 + \gamma^{55}_{44}(v_4)^2(l_5)^2 + \gamma^{44}_{45}v_4v_5(l_4)^2\\
&\quad + \gamma^{45}_{45}v_4v_5l_4l_5 + \gamma^{55}_{45}v_4v_5(l_5)^2 + \gamma^{44}_{55}(v_5)^2(l_4)^2\\
&\quad + \gamma^{45}_{55}(v_5)^2l_4l_5 + \gamma^{55}_{55}(v_5)^2(l_5)^2][M-k^2]\\
&\quad - [D_0 + \beta_4v_4 + \beta_5v_5 + \delta_{44}(v_4)^2 + \delta_{45}v_4v_5\\
&\quad + \delta_{55}(v_5)^2 + \delta^{44}(l_4)^2 + \delta^{45}l_4l_5 + \delta^{55}(l_5)^2\\
&\quad + \delta_{444}(v_4)^3 + \delta_{445}(v_4)^2v_5 + \delta_{455}v_4(v_5)^2\\
&\quad + \delta_{555}(v_5)^3 + \delta^{44}_4 v_4(l_4)^2 + \delta^{45}_4 v_4l_4l_5\\
&\quad + \delta^{55}_4 v_4(l_5)^2 + \delta^{44}_5 v_5(l_4)^2 + \delta^{45}_5 v_5l_4l_5\\
&\quad + \delta^{55}_5 v_5(l_5)^2][M-k^2]^2\\
&\quad + [H_0 + h_4v_4 + h_5v_5][M-k^2]^3 \qquad (3)
\end{aligned}$$

Vibration and rotation l-type resonances are expressed by off-diagonal matrix elements (see Table 1 of Ref. [24]) containing the following parameters:

$$\begin{aligned}
r_{45} &= r^0_{45} + r_{445}(v_4+1) + r_{455}(v_5+1) + r^J_{45}M + r^{JJ}_{45}M^2\\
&\quad + r^{JJJ}_{45}M^3 + r_{4445}(v_4+1)^2 + r_{4455}(v_4+1)(v_5+1)\\
&\quad + r_{4555}(v_5+1)^2 + r^J_{445}(v_4+1)M + r^J_{455}(v_5+1)
\end{aligned} \quad (4)$$

$$\begin{aligned}
q_t &= q^0_t + q_{tt}v_t + q_{tt'}v_{t'} + q_{ttt}(v_t)^2 + q^J_tM + q^{JJ}_tM^2\\
&\quad + q^{JJJ}_tM^3 + q^J_{tt}v_tM + q^{JJ}_{tt}v_tM^2 + q^k_t(k\pm1)^2
\end{aligned} \quad (5)$$

$$\rho_t = \rho^0_t + \rho_{tt}v_t + \rho_{tt'}v_{t'} + \rho_{ttt}(v_t)^2 + \rho^J_tM + \rho^J_{tt}v_tM \quad (6)$$

$$\rho^0_{45} + \rho^0_{454}v_4 + \rho^0_{455}v_5 + \rho^{0J}_{45}M, \quad (7)$$

with $M=J(J+1)$, and t, $t'=4$ or 5.

Some terms of higher order in the expansion of the Hamiltonian have not been included in the previous equations since they were not determinable in the least-squares analysis.

The analysis of all the assigned transitions was performed in several steps. First, after having extended the J range of the transitions of all the bands previously reported [6], in particular those of the $v_4=2$ manifold (Σ^+ and Δ states), all the data

Table 1. Bands of $^{13}C_2H_2$ included in the least-squares fitting procedures.

Vibrational transition	Symmetry	ν_C[a]	Assigned transitions	$\sigma(\times10^5)$[b]
(a) 60–250 cm^{-1}				
$\nu_5 \leftarrow \nu_4$	$\Pi_u \leftarrow \Pi_g$	124.46284	$P_{e\text{-}e}$ (2-28); $R_{e\text{-}e}$ (1-45); $Q_{f\text{-}e}$ (1-18) $P_{f\text{-}f}$ (2-28); $R_{f\text{-}f}$ (1-43); $Q_{e\text{-}f}$ (1-16)	8
$\nu_4+\nu_5 \leftarrow 2\nu_4$	$\Sigma_u^+ \leftarrow \Sigma_g^+$	104.98955	$P_{e\text{-}e}$ (1-17); $R_{e\text{-}e}$ (0-32)	6
	$(\Delta_{u(e)} \leftarrow \Sigma_g^+)$[c]	119.91754	$P_{e\text{-}e}$ (6-23); $R_{e\text{-}e}$ (4-38)	7
	$\Delta_u \leftarrow \Delta_g$	121.19357	$P_{e\text{-}e}$ (3-25); $R_{e\text{-}e}$ (2-34); $Q_{f\text{-}e}$ (2-17) $P_{f\text{-}f}$ (3-25); $R_{f\text{-}f}$ (2-38); $Q_{e\text{-}f}$ (2-17)	11
$2\nu_5 \leftarrow \nu_4+\nu_5$	$\Sigma_g^+ \leftarrow \Sigma_u^+$	128.05076	$P_{e\text{-}e}$ (1-27); $R_{e\text{-}e}$ (0-35)	6
	$\Delta_g \leftarrow \Delta_u$	122.37800	$P_{e\text{-}e}$ (3-23); $R_{e\text{-}e}$ (2-35); $Q_{f\text{-}e}$ (2-14) $P_{f\text{-}f}$ (3-25); $R_{f\text{-}f}$ (2-36); $Q_{e\text{-}f}$ (2-12)	10
$2\nu_4+\nu_5 \leftarrow 3\nu_4$	$^{II}\Pi_u \leftarrow \Pi_g$	92.92980	$P_{e\text{-}e}$ (3-12); $R_{e\text{-}e}$ (1-27); $Q_{f\text{-}e}$ (1,2) $P_{f\text{-}f}$ (2-11); $R_{f\text{-}f}$ (1-27)	20
	$(^{II}\Pi_u \leftarrow \Phi_g)$[c]	95.53632	$P_{e\text{-}e}$ (12); $R_{e\text{-}e}$ (10-26); $R_{f\text{-}f}$ (14-21)	18
	$^{I}\Pi_u \leftarrow \Pi_g$	112.51685	$P_{e\text{-}e}$ (2-11); $R_{e\text{-}e}$ (4-16) $P_{f\text{-}f}$ (7-11); $R_{f\text{-}f}$ (2-19)	19
	$(\Phi_u \leftarrow \Pi_g)$[c]	115.33620	$P_{e\text{-}e}$ (12-14); $R_{e\text{-}e}$ (11-26) $P_{f\text{-}f}$ (12-17); $R_{f\text{-}f}$ (12-25)	24
	$(^{I}\Pi_u \leftarrow \Phi_g)$[c]	115.12338	$R_{e\text{-}e}$ (12-25); $R_{f\text{-}f}$ (11-21)	17
	$\Phi_u \leftarrow \Phi_g$	117.94273	$P_{e\text{-}e}$ (4-17); $R_{e\text{-}e}$ (3-18); $Q_{f\text{-}e}$ (3-12) $P_{f\text{-}f}$ (4-19); $R_{f\text{-}f}$ (3-24); $Q_{e\text{-}f}$ (3-12)	16
$\nu_4+2\nu_5 \leftarrow 2\nu_4+\nu_5$	$^{II}\Pi_g \leftarrow {}^{II}\Pi_u$	115.06476	$P_{e\text{-}e}$ (3-18); $R_{e\text{-}e}$ (1-28); $Q_{f\text{-}e}$ (1) $P_{f\text{-}f}$ (2-20); $R_{f\text{-}f}$ (2-30); $Q_{e\text{-}f}$ (1,2)	21
	$^{II}\Pi_g \leftarrow {}^{I}\Pi_u$	95.47770	$P_{e\text{-}e}$ (5-13); $R_{e\text{-}e}$ (1-21) $P_{f\text{-}f}$ (2-11); $R_{f\text{-}f}$ (2-20)	19
	$^{I}\Pi_g \leftarrow {}^{I}\Pi_u$	113.21417	$P_{e\text{-}e}$ (2-13); $R_{e\text{-}e}$ (2-22) $P_{f\text{-}f}$ (6-13); $R_{f\text{-}f}$ (10-22)	20
	$\Phi_g \leftarrow \Phi_u$	119.31230	$P_{e\text{-}e}$ (4-20); $R_{e\text{-}e}$ (3-26); $Q_{f\text{-}e}$ (3-13) $P_{f\text{-}f}$ (4-20); $R_{f\text{-}f}$ (3-26); $Q_{e\text{-}f}$ (3-14)	18
$3\nu_5 \leftarrow \nu_4+2\nu_5$	$\Pi_u \leftarrow {}^{II}\Pi_g$	128.25036	$P_{e\text{-}e}$ (2-18); $R_{e\text{-}e}$ (1-26) $P_{f\text{-}f}$ (2-15); $R_{f\text{-}f}$ (1-26)	19
	$\Phi_u \leftarrow \Phi_g$	120.04693	$P_{e\text{-}e}$ (4-17); $R_{e\text{-}e}$ (3-25) $P_{f\text{-}f}$ (4-16); $R_{f\text{-}f}$ (3-25)	16
(b) 400–600 cm^{-1}				
$2\nu_4 \leftarrow \nu_5$	$\Sigma_g^+ \leftarrow \Pi_u$	485.01967	$P_{e\text{-}e}$ (1-33); $R_{e\text{-}e}$ (1-35); $Q_{f\text{-}e}$ (1-30)	10
	$\Delta_g \leftarrow \Pi_u$	483.74364	$P_{e\text{-}e}$ (3-12); $R_{e\text{-}e}$ (1-12); $Q_{f\text{-}e}$ (2-32) $P_{f\text{-}f}$ (3-25); $R_{f\text{-}f}$ (1-26); $Q_{e\text{-}f}$ (2-34)	11
$3\nu_4 \leftarrow \nu_4+\nu_5$	$\Pi_g \leftarrow \Sigma_u^+$	510.04387	$P_{e\text{-}e}$ (5-17); $R_{e\text{-}e}$ (4-13); $Q_{f\text{-}e}$ (2-15)	24
	$\Pi_g \leftarrow \Sigma_u^-$	497.67269	$P_{e\text{-}e}$ (2-26); $R_{e\text{-}e}$ (0-25); $Q_{e\text{-}f}$ (1-30)	15
	$\Pi_g \leftarrow \Delta_u$	495.11588	$P_{e\text{-}e}$ (2-23); $R_{e\text{-}e}$ (1-23); $Q_{f\text{-}e}$ (2-22) $P_{f\text{-}f}$ (2-24); $R_{f\text{-}f}$ (3-25); $Q_{e\text{-}f}$ (2-15)	17
	$\Phi_g \leftarrow \Delta_u$	492.50936	$P_{e\text{-}e}$ (6-11); $R_{e\text{-}e}$ (2-17); $Q_{f\text{-}e}$ (5-28) $P_{f\text{-}f}$ (5-16); $R_{f\text{-}f}$ (2-21); $Q_{e\text{-}f}$ (4-26)	19
$2\nu_4+\nu_5 \leftarrow 2\nu_5$	$^{I}\Pi_u \leftarrow \Sigma_g^+$	494.50996	$P_{e\text{-}e}$ (2-23); $R_{e\text{-}e}$ (0-19);$Q_{f\text{-}e}$ (1-23)	22
	$^{I}\Pi_u \leftarrow \Delta_g$	485.25474	$P_{e\text{-}e}$ (10-16); $Q_{f\text{-}e}$ (2-23) $Q_{e\text{-}f}$ (2-21)	23
	$\Phi_u \leftarrow \Delta_g$	488.07409	$P_{e\text{-}e}$ (9-18); $R_{e\text{-}e}$ (2-21); $Q_{f\text{-}e}$ (3-20) $P_{f\text{-}f}$ (5-16); $R_{f\text{-}f}$ (2-17); $Q_{e\text{-}f}$ (3-19)	24
(c) 600–800 cm^{-1}				
$\nu_5 \leftarrow$ G.S.	$\Pi_u \leftarrow \Sigma_g^+$	727.23019	$P_{e\text{-}e}$ (2-54); $R_{e\text{-}e}$ (0-50); $Q_{f\text{-}e}$ (1-53)	7
$\nu_4+\nu_5 \leftarrow \nu_4$	$\Sigma_u^+ \leftarrow \Pi_g$	714.47207	$P_{e\text{-}e}$ (1-48); $R_{e\text{-}e}$ (1-42); $Q_{e\text{-}f}$ (5-41)	9
	$\Sigma_u^- \leftarrow \Pi_g$	726.84325	$P_{f\text{-}f}$ (1-43); $R_{f\text{-}f}$ (1-41); $Q_{f\text{-}e}$ (1-43)	11
	$\Delta_u \leftarrow \Pi_g$	729.40006	$P_{e\text{-}e}$ (3-41); $R_{e\text{-}e}$ (1-40); $Q_{f\text{-}e}$ (2-42) $P_{f\text{-}f}$ (3-43); $R_{f\text{-}f}$ (1-40); $Q_{e\text{-}f}$ (2-44)	11
$2\nu_5 \leftarrow \nu_5$	$\Sigma_g^+ \leftarrow \Pi_u$	718.05999	$P_{e\text{-}e}$ (1-45) $R_{e\text{-}e}$ (1-43); $Q_{e\text{-}f}$ (6-42)	9
	$\Delta_g \leftarrow \Pi_u$	727.31521	$P_{e\text{-}e}$ (3-42); $R_{e\text{-}e}$ (1-39); $Q_{e\text{-}f}$ (5-37) $P_{f\text{-}f}$ (3-44); $R_{f\text{-}f}$ (1-42); $Q_{f\text{-}e}$ (2-44)	9
$2\nu_4+\nu_5 \leftarrow 2\nu_4$	$^{II}\Pi_u \leftarrow \Sigma_g^+$	707.96322	$P_{e\text{-}e}$ (2-22); $R_{e\text{-}e}$ (0-20);$Q_{e\text{-}f}$ (1-32)	18

(*continued*)

Table 1. Continued.

Vibrational transition	Symmetry	ν_C[a]	Assigned transitions	$\sigma(\times 10^5)$[b]
	$^{II}\Pi_u \leftarrow \Delta_g$	709.23925	$P_{e\text{-}e}$ (3-36); $R_{e\text{-}e}$ (2-32); $Q_{e\text{-}f}$ (2-35) $P_{f\text{-}f}$ (2-38); $R_{f\text{-}f}$ (4-32); $Q_{f\text{-}e}$ (2-34)	17
	$^{I}\Pi_u \leftarrow \Sigma_g^+$	727.55028	$P_{e\text{-}e}$ (2-35); $R_{e\text{-}e}$ (1-29); $Q_{e\text{-}f}$ (4-33)	18
	$^{I}\Pi_u \leftarrow \Delta_g$	728.82631	$P_{e\text{-}e}$ (2-29); $R_{e\text{-}e}$ (2-30) $P_{f\text{-}f}$ (2-30); $R_{f\text{-}f}$ (2-18)	18
	$\Phi_u \leftarrow \Delta_g$	731.64566	$P_{e\text{-}e}$ (4-28); $R_{e\text{-}e}$ (2-27); $Q_{e\text{-}f}$ (4-29) $P_{f\text{-}f}$ (4-29); $R_{f\text{-}f}$ (2-29); $Q_{f\text{-}e}$ (4-27)	19
$\nu_4+2\nu_5 \leftarrow \nu_4+\nu_5$	$^{II}\Pi_g \leftarrow \Sigma_u^+$	718.03843	$P_{e\text{-}e}$ (2-36); $R_{e\text{-}e}$ (0-33); $Q_{f\text{-}e}$ (1-33)	18
	$^{II}\Pi_g \leftarrow \Sigma_u^-$	705.66725	$P_{f\text{-}f}$ (3-31); $R_{f\text{-}f}$ (0-24); $Q_{e\text{-}f}$ (1-28)	19
	$^{II}\Pi_g \leftarrow \Delta_u$	703.11044	$P_{e\text{-}e}$ (2-32); $R_{e\text{-}e}$ (2-24); $Q_{e\text{-}f}$ (2-32) $P_{f\text{-}f}$ (2-32); $R_{f\text{-}f}$ (2-26); $Q_{f\text{-}e}$ (2-28)	18
	$^{I}\Pi_g \leftarrow \Sigma_u^+$	735.77490	$P_{e\text{-}e}$ (4-27); $R_{e\text{-}e}$ (1-20); $Q_{f\text{-}e}$ (2-29)	24
	$^{I}\Pi_g \leftarrow \Sigma_u^-$	723.40372	$P_{f\text{-}f}$ (2-39); $R_{f\text{-}f}$ (0-34); $Q_{e\text{-}f}$ (1-31)	15
	$^{I}\Pi_g \leftarrow \Delta_u$	720.84691	$P_{e\text{-}e}$ (2-32); $R_{e\text{-}e}$ (4-29); $Q_{e\text{-}f}$ (2-30) $P_{f\text{-}f}$ (2-36); $R_{f\text{-}f}$ (6-32); $Q_{f\text{-}e}$ (10-30)	17
	$\Phi_g \leftarrow \Delta_u$	729.76438	$P_{e\text{-}e}$ (4-32); $R_{e\text{-}e}$ (2-29); $Q_{e\text{-}f}$ (4-30) $P_{f\text{-}f}$ (4-28); $R_{f\text{-}f}$ (2-30); $Q_{f\text{-}e}$ (4-31)	19
$3\nu_5 \leftarrow 2\nu_5$	$\Pi_u \leftarrow \Sigma_g^+$	718.23802	$P_{e\text{-}e}$ (2-39); $R_{e\text{-}e}$ (0-34); $Q_{f\text{-}e}$ (1-33)	11
	$\Pi_u \leftarrow \Delta_g$	708.98279	$P_{e\text{-}e}$ (2-32); $R_{e\text{-}e}$ (2-25); $Q_{e\text{-}f}$ (2-35) $P_{f\text{-}f}$ (2-38); $R_{f\text{-}f}$ (3-31); $Q_{f\text{-}e}$ (2-35)	13
	$\Phi_u \leftarrow \Delta_g$	727.43332	$P_{e\text{-}e}$ (4-28); $R_{e\text{-}e}$ (2-28); $Q_{e\text{-}f}$ (4-27) $P_{f\text{-}f}$ (4-31); $R_{f\text{-}f}$ (2-29); $Q_{f\text{-}e}$(4-30)	16
$3\nu_4+\nu_5 \leftarrow 3\nu_4$	$\Sigma_u^+ \leftarrow \Pi_g$	704.32983	$P_{e\text{-}e}$ (1-27); $R_{e\text{-}e}$ (1-23); $Q_{e\text{-}f}$(1-27)	32
	$\Sigma_u^- \leftarrow \Pi_g$	727.51244	$P_{f\text{-}f}$ (2-19); $R_{f\text{-}f}$ (1-15); $Q_{f\text{-}e}$(1-26)	43
	$^{II}\Delta_u \leftarrow \Pi_g$	700.79637	$P_{e\text{-}e}$ (3-16); $R_{e\text{-}e}$ (1-19); $Q_{e\text{-}f}$ (2-17) $P_{f\text{-}f}$ (3-15); $R_{f\text{-}f}$ (2-18); $Q_{f\text{-}e}$(3-30)	34
	$^{II}\Delta_u \leftarrow \Phi_g$	703.40290	$P_{e\text{-}e}$ (3-31); $R_{e\text{-}e}$ (3-21); $Q_{e\text{-}f}$ (3-31) $P_{f\text{-}f}$ (3-33); $R_{f\text{-}f}$ (3-21); $Q_{f\text{-}e}$(3-30)	30
$2\nu_4+2\nu_5 \leftarrow 2\nu_4+\nu_5$	$^{II}\Sigma_g^+ \leftarrow {}^{I}\Pi_u$	686.63301	$P_{e\text{-}e}$ (5-16); $R_{e\text{-}e}$ (5-16); $Q_{e\text{-}f}$ (1-16)	37
	$^{I}\Sigma_g^+ \leftarrow {}^{I}\Pi_u$	722.40721	$Q_{e\text{-}f}$ (6-13)	197
	$\Sigma_g^- \leftarrow {}^{I}\Pi_u$	699.65861	$P_{f\text{-}f}$ (1-24); $R_{f\text{-}f}$ (1-22)); $Q_{f\text{-}e}$(1-28)	28
	$^{II}\Delta_g \leftarrow {}^{II}\Pi_u$	719.87703	$P_{e\text{-}e}$ (3-26); $R_{e\text{-}e}$ (1-15); $Q_{e\text{-}f}$ (2-22) $P_{f\text{-}f}$ (3-24); $R_{f\text{-}f}$ (1-14); $Q_{f\text{-}e}$ (2-30)	33
	$^{II}\Delta_g \leftarrow {}^{I}\Pi_u$	700.28998	$P_{e\text{-}e}$ (3-29); $R_{e\text{-}e}$ (1-21); $Q_{e\text{-}f}$ (6-18) $P_{f\text{-}f}$ (3-30); $R_{f\text{-}f}$ (1-22);	33
	$^{II}\Delta_g \leftarrow \Phi_u$	697.47063	$P_{e\text{-}e}$ (3-26); $R_{e\text{-}e}$ (3-24); $Q_{e\text{-}f}$ (3-30) $P_{f\text{-}f}$ (3-25); $R_{f\text{-}f}$ (3-22); $Q_{f\text{-}e}$ (3-24)	37
	$^{I}\Delta_g \leftarrow {}^{I}\Pi_u$	726.45373	$P_{e\text{-}e}$ (3-22); $R_{e\text{-}e}$ (1-22); $Q_{e\text{-}f}$ (2-20) $P_{f\text{-}f}$ (3-24); $R_{f\text{-}f}$ (1-20); $Q_{f\text{-}e}$ (2-15)	35
	$^{II}\Sigma_g^+ \leftarrow {}^{II}\Pi_u$	706.22007	$P_{e\text{-}e}$ (2-33); $R_{e\text{-}e}$ (2-26); $Q_{e\text{-}f}$ (1-28)	25
	$\Sigma_g^- \leftarrow {}^{II}\Pi_u$	719.24567	$P_{f\text{-}f}$ (1-32); $R_{f\text{-}f}$ (1-25); $Q_{f\text{-}e}$ (1-28)	27
$\nu_4+3\nu_5 \leftarrow \nu_4+2\nu_5$	$\Sigma_u^+ \leftarrow {}^{II}\Pi_g$	708.14320	$P_{e\text{-}e}$ (1-24); $R_{e\text{-}e}$ (1-23); $Q_{e\text{-}f}$ (1-23)	31
	$\Sigma_u^- \leftarrow {}^{II}\Pi_g$	733.68404	$P_{f\text{-}f}$ (5-20); $R_{f\text{-}f}$ (1-11); $Q_{f\text{-}e}$ (1-9)	49
	$^{II}\Delta_u \leftarrow {}^{II}\Pi_g$	718.90128	$P_{e\text{-}e}$ (3-26); $R_{e\text{-}e}$ (1-20); $Q_{e\text{-}f}$ (2-27) $P_{f\text{-}f}$ (3-29); $R_{f\text{-}f}$ (1-26); $Q_{f\text{-}e}$ (2-29)	36
	$\Sigma_u^+ \leftarrow {}^{I}\Pi_g$	690.40673	$P_{e\text{-}e}$ (1-23); $R_{e\text{-}e}$ (1-19); $Q_{e\text{-}f}$ (1-20)	40
	$\Sigma_u^- \leftarrow {}^{I}\Pi_g$	715.94757	$Q_{f\text{-}e}$ (6-19)	37
	$^{II}\Delta_u \leftarrow \Phi_g$	692.24734	$P_{e\text{-}e}$ (3-22); $R_{e\text{-}e}$ (3-23); $Q_{e\text{-}f}$ (3-25) $P_{f\text{-}f}$ (3-27); $R_{f\text{-}f}$ (3-26); $Q_{f\text{-}e}$ (3-27)	31
$4\nu_5 \leftarrow 3\nu_5$	$\Sigma_g^+ \leftarrow \Pi_u$	709.26237	$P_{e\text{-}e}$ (1-33); $R_{e\text{-}e}$ (3-24); $Q_{e\text{-}f}$ (1-27)	27
	$\Delta_g \leftarrow \Pi_u$	718.45162	$P_{e\text{-}e}$ (3-26); $R_{e\text{-}e}$ (1-15); $Q_{e\text{-}f}$ (2-23) $P_{f\text{-}f}$ (4-23); $R_{f\text{-}f}$ (1-19); $Q_{f\text{-}e}$ (2-26)	30
	$\Delta_g \leftarrow \Phi_u$	700.00110	$P_{e\text{-}e}$ (3-26); $R_{e\text{-}e}$ (3-19); $Q_{e\text{-}f}$ (2-31) $P_{f\text{-}f}$ (3-25); $R_{f\text{-}f}$ (4-22); $Q_{f\text{-}e}$ (2-26)	31
	$\Gamma_g \leftarrow \Phi_u$	727.58894	$P_{e\text{-}e}$ (5-30); $R_{e\text{-}e}$ (3-25); $Q_{e\text{-}f}$ (9,12) $P_{f\text{-}f}$ (5-29); $R_{f\text{-}f}$ (3-21); $Q_{f\text{-}e}$ (5-17)	40
(d) 1200–1400 cm^{-1}				
$\nu_4+\nu_5 \leftarrow$ G.S.	$\Sigma_u^+ \leftarrow \Sigma_g^+$	1317.23941	$P_{e\text{-}e}$ (1-47); $R_{e\text{-}e}$ (0-44)	18
	$(\Delta_{u(e)} \leftarrow \Sigma_g^+)$[c]	1332.16740	$P_{e\text{-}e}$ (7-41); $R_{e\text{-}e}$ (7-39)	34

(*continued*)

Table 1. Continued.

Vibrational transition	Symmetry	ν_C[a]	Assigned transitions	$\sigma(\times 10^5)$[b]
$2\nu_4+\nu_5 \leftarrow \nu_4$	$^{II}\Pi_u \leftarrow \Pi_g$	1317.44574	$P_{e\text{-}e}$ (2-37); $R_{e\text{-}e}$ (1-37); $Q_{e\text{-}f}$ (1-15) $P_{f\text{-}f}$ (2-41); $R_{f\text{-}f}$ (1-37);$Q_{f\text{-}e}$(1-22)	26
	$^{I}\Pi_u \leftarrow \Pi_g$	1337.03279	$P_{e\text{-}e}$ (3-14); $R_{e\text{-}e}$ (4-14) $P_{f\text{-}f}$ (2-25); $R_{f\text{-}f}$ (2-23)	33
$\nu_4+2\nu_5 \leftarrow \nu_5$	$^{II}\Pi_g \leftarrow \Pi_u$	1308.04765	$P_{e\text{-}e}$ (2-37); $R_{e\text{-}e}$ (1-35); $Q_{e\text{-}f}$ (1-20) $P_{f\text{-}f}$ (2-38); $R_{f\text{-}f}$ (1-36); $Q_{f\text{-}e}$(1-16)	26
	$^{I}\Pi_g \leftarrow \Pi_u$	1325.78412	$P_{e\text{-}e}$ (2-24); $R_{e\text{-}e}$ (2-21) $P_{f\text{-}f}$ (2-22); $R_{f\text{-}f}$ (1-23)	33
$3\nu_4+\nu_5 \leftarrow 2\nu_4$	$\Sigma_u^+ \leftarrow \Sigma_g^+$	1319.36326	$P_{e\text{-}e}$ (1-32); $R_{e\text{-}e}$ (0-29)	33
	$^{II}\Delta_u \leftarrow \Delta_g$	1317.10583	$P_{e\text{-}e}$ (3-29); $R_{e\text{-}e}$ (2-30) $P_{f\text{-}f}$ (3-31); $R_{f\text{-}f}$ (2-30)	35
$2\nu_4+2\nu_5 \leftarrow \nu_4+\nu_5$	$^{II}\Sigma_g^+ \leftarrow \Sigma_u^+$	1309.19373	$P_{e\text{-}e}$ (1-32); $R_{e\text{-}e}$ (0-32)	28
	$\Sigma_g^- \leftarrow \Sigma_u^-$	1309.84815	$P_{f\text{-}f}$ (1-30); $R_{f\text{-}f}$ (0-30))	23
	$^{II}\Delta_g \leftarrow \Delta_u$	1307.92271	$P_{e\text{-}e}$ (3-29); $R_{e\text{-}e}$ (2-31) $P_{f\text{-}f}$ (3-31); $R_{f\text{-}f}$ (2-28)	42
$\nu_4+3\nu_5 \leftarrow 2\nu_5$	$\Sigma_u^+ \leftarrow \Sigma_g^+$	1298.13086	$P_{e\text{-}e}$ (1-28); $R_{e\text{-}e}$ (0-26)	30
	$^{II}\Delta_u \leftarrow \Delta_g$	1299.63372	$P_{e\text{-}e}$ (3-30); $R_{e\text{-}e}$ (2-29); $Q_{e\text{-}f}$ (2-10) $P_{f\text{-}f}$ (3-29); $R_{f\text{-}f}$ (2-27); $Q_{f\text{-}e}$(2-12)	38
(e) 1800–2200 cm^{-1}				
$2\nu_4+\nu_5 \leftarrow$ G.S.	$^{II}\Pi_u \leftarrow \Sigma_g^+$	1920.21308	$P_{e\text{-}e}$ (2-34); $R_{e\text{-}e}$ (0-32); $Q_{f\text{-}e}$ (1-35)	20
	$^{I}\Pi_u \leftarrow \Sigma_g^+$	1939.80014	$P_{e\text{-}e}$ (3-28); $R_{e\text{-}e}$ (0-29); $Q_{f\text{-}e}$ (1-30)	21
$3\nu_5 \leftarrow$ G.S.	$\Pi_u \leftarrow \Sigma_g^+$	2163.52819	$P_{e\text{-}e}$ (2-36); $R_{e\text{-}e}$ (0-34); $Q_{f\text{-}e}$ (1-34)	18
$3\nu_4+\nu_5 \leftarrow \nu_4$	$\Sigma_u^+ \leftarrow \Pi_g$	1928.84578	$P_{e\text{-}e}$ (1-16); $R_{e\text{-}e}$ (1-12); $Q_{e\text{-}f}$ (1-29)	39
	$\Sigma_u^- \leftarrow \Pi_g$	1952.02830	$Q_{f\text{-}e}$ (1-21)	41
	$^{II}\Delta_u \leftarrow \Pi_g$	1925.31231	$P_{e\text{-}e}$ (3-28); $R_{e\text{-}e}$ (1-27); $Q_{e\text{-}f}$ (6-22) $P_{f\text{-}f}$ (3-26); $R_{f\text{-}f}$ (1-25); $Q_{f\text{-}e}$ (3-28)	38
$2\nu_4+2\nu_5 \leftarrow \nu_5$	$^{II}\Sigma_g^+ \leftarrow \Pi_u$	1899.20296	$P_{e\text{-}e}$ (1-23); $R_{e\text{-}e}$ (1-21); $Q_{e\text{-}f}$ (5-16)	41
	$^{I}\Sigma_g^+ \leftarrow \Pi_u$	1934.97716	$Q_{e\text{-}f}$ (4-20)	185
	$\Sigma_g^- \leftarrow \Pi_u$	1912.22856	$P_{f\text{-}f}$ (1-22); $R_{f\text{-}f}$ (1-19); $Q_{f\text{-}e}$ (1-29)	34
	$^{II}\Delta_g \leftarrow \Pi_u$	1912.85993	$P_{e\text{-}e}$ (5-16); $R_{e\text{-}e}$ (1-14); $Q_{f\text{-}e}$ (2-18) $P_{f\text{-}f}$ (3-22); $R_{f\text{-}f}$ (1-21); $Q_{e\text{-}f}$ (2-20)	45
$\nu_4+3\nu_5 \leftarrow \nu_4$	$\Sigma_u^+ \leftarrow \Pi_g$	2140.65369	$P_{e\text{-}e}$ (1-24); $R_{e\text{-}e}$ (1-19); $Q_{e\text{-}f}$ (1-21)	41
	$\Sigma_u^- \leftarrow \Pi_g$	2166.19454	$P_{f\text{-}f}$ (2-25); $R_{f\text{-}f}$ (2-23)); $Q_{f\text{-}e}$(1-22)	44
	$^{II}\Delta_u \leftarrow \Pi_g$	2151.41178	$P_{e\text{-}e}$ (3-20); $R_{e\text{-}e}$ (1-19); $Q_{f\text{-}e}$ (2-22) $P_{f\text{-}f}$ (4-21); $R_{f\text{-}f}$ (1-17); $Q_{e\text{-}f}$ (2-22)	43
$4\nu_5 \leftarrow \nu_5$	$\Sigma_g^+ \leftarrow \Pi_u$	2145.56038	$P_{e\text{-}e}$ (1-28); $R_{e\text{-}e}$ (1-28); $Q_{e\text{-}f}$ (1-19)	38
	$\Delta_g \leftarrow \Pi_u$	2154.74963	$P_{e\text{-}e}$ (3-22); $R_{e\text{-}e}$ (1-22); $Q_{e\text{-}f}$ (2-30) $P_{f\text{-}f}$ (4-26); $R_{f\text{-}f}$ (1-25); $Q_{f\text{-}e}$ (2-25)	35
(f) 2300–2700 cm^{-1}				
$3\nu_4+\nu_5 \leftarrow$ G.S.	$\Sigma_u^+ \leftarrow \Sigma_g^+$	2531.61312	$P_{e\text{-}e}$ (1-30); $R_{e\text{-}e}$ (0-30)	33
	$(^{II}\Delta_{u(e)} \leftarrow \Sigma_g^+)$[c]	2528.07966	$P_{e\text{-}e}$ (9-27); $R_{e\text{-}e}$ (9-26)	39

[a]For the definition of the band centre, ν_C, see text.
[b]σ (cm^{-1}) corresponds to the RMS value of the residuals for the various assigned lines resulting from the simultaneous fits (see text).
[c]Perturbation allowed transition.

involving states up to $v_{tot}=2$ were fitted simultaneously, using as starting parameters the values in Table VI of Ref. [6]. The subsequent steps consisted in the addition to the $v_{tot}=2$ data set of all the transitions measured in the FIR region, involving states of one $v_{tot}=3$ manifold at a time. New parameters or rotation and/or vibration dependences of the previously determined constants, characterizing the investigated manifold, were refined. After each fit the statistical significance of the obtained parameters was checked as well as the correlation coefficients between them. The results of the simultaneous analysis were compared to those obtained in the single band fits previously mentioned to test their quality and the adequacy of the model.

The weights of the experimental data were chosen proportional to the inverse of their squared estimated uncertainties. An uncertainty similar to the RMS value

of the single band fit ($2.0/3.0 \times 10^{-4}\,cm^{-1}$) was assigned to all the measured wavenumbers, despite the fact that the lines had different S/N depending on their intensity and on the experimental conditions in the various spectral regions. Finally, all the transition wavenumbers that differed from their corresponding calculated values by more than twice the uncertainty of the measurements were excluded from the data set in the final cycle of the analysis.

From the analysis of the 5874 transitions involving states up to $v_{tot} = 3$ a total of 80 parameters, which are listed in Table 2, were determined. They reproduce 5605 observed wavenumbers with a RMS error of $1.75 \times 10^{-4}\,cm^{-1}$, of the same order of the experimental uncertainty. In the final cycle of the analysis 269 (4.6%) transitions were discarded according to the above-mentioned criterion for rejection. The RMS error for each band is reported in the last column of Table 1. The transitions involving the $v_4 = 1$, $v_5 = 2$, $^{II}\Pi_g$ (f) levels are perturbed. They were satisfactorily reproduced only by adding a set of effective q-type parameters in the model, see Equation (5), q_{44}^{12}, q_{55}^{12}, q_{44J}^{12}, q_{55J}^{12} and q_{44JJ}^{12}, which contribute only to the energy of the levels for this manifold. Nevertheless, the transitions to (f) levels for $J \geq 26$ are discarded in the fit.

Similarly, the values of $v_4 = 2$, $v_5 = 1$, Φ_u (f) levels are more and more underestimated with increasing J. All the parameters of the model listed in Equations (2) to (7) not present in Table 2 were nevertheless allowed to vary during the fitting procedure but they resulted statistically undetermined. All the 19 states of the various manifold up to $v_{tot} = 3$ were characterized.

The $v_{tot} = 4$ manifolds were then added to the previous data set adopting the same criteria used for the analysis of the $v_{tot} = 3$ manifolds. Although higher order parameters were added to those in Table 2, large discrepancies between observed and calculated transition wavenumbers were noticed. In addition, anomalous and poorly determined values of several parameters were obtained. Different sets of constants were refined but none were able to reproduce satisfactorily the experimental data. The perturbation of the energies of the $v_{tot} = 4$ levels could be ascribed to the effects of rotation–vibration interactions between levels belonging to different manifolds, which are not taken into account in our model. In addition, transitions involving the $v_4 = 4$ manifold and a few states belonging to other manifolds were not observed. It should be remembered that the density of states increases with increasing energy, favouring interactions of different kinds between the excited levels. Similar perturbations were also present in the spectra involving the $v_{tot} = 4$ levels of $^{12}C_2H_2$ and were ascribed to interactions with the $v_2 = v_4 = 1$ or $v_2 = v_5 = 1$ states [23]. An analogous explanation is plausible also for the presently investigated molecule, taking into account that the energies of the corresponding levels are very similar in the two molecules.

A different strategy was then chosen for the analysis, fitting only the transitions belonging to one $v_{tot} = 4$ manifold at a time to a set of effective higher order constants. These were added to the ones already determined from the previous analysis, which were constrained to the values in Table 2. This procedure has the advantage of preserving the physical significance of the parameters characterizing the states up to $v_{tot} = 3$ from the effects of the perturbations affecting only the energies of the $v_{tot} = 4$ manifolds. The same weighting scheme as for the analysis of the $v_{tot} = 3$ levels was adopted, assigning the same uncertainty to all the measured lines belonging to the same band. However, the limit for rejection of the experimental data was increased in order to avoid the exclusion of too many transitions or of most of the transitions of a given branch, which would have prevented the determination of a few refining parameters. For all the manifolds, the value of $1.0 \times 10^{-3}\,cm^{-1}$ was chosen, with the exception of two bands in the $v_4 = 2$, $v_5 = 2$ manifold for which a larger limit ($5.0 \times 10^{-3}\,cm^{-1}$) was adopted.

Table 3 lists the four sets of effective constants obtained with the procedure described above. The standard deviations of the fits for the bands belonging to the $v_{tot} = 4$ manifolds are about twice as large as that obtained in the simultaneous analysis of $v_{tot} = 3$ bands, the value for the bands of the $v_4 = 2$, $v_5 = 2$ manifold being slightly higher, notwithstanding the introduction of 21 parameters in the fitting procedure. As can be seen in Table 1, the RMS error for each band in the various manifolds parallels the behaviour of the standard deviation of the fits. It should be remembered that the parameters in Table 3 are effective ones, perhaps with the exception of those for the $v_4 = 0$, $v_5 = 4$ manifold. This is particularly evident for the parameters common to different manifolds, for instance q_{444}, q_{555} and q_{44}^J, whose values differ by orders of magnitude in the various sets. Moreover, most of the parameters have anomalous values, being of the same order of magnitude or larger than the corresponding lower order constants in Table 2. Nevertheless, by means of these parameters it has been possible to predict and fit new transitions in a particularly dense region of the spectrum.

In total, 9529 $\Delta J = 0, \pm 1$ transitions of 101 vibration–rotation bands connecting 32 bending state, whose energies are reported in Table 4, were identified and fitted.

Table 2. Spectroscopic parameters (in cm^{-1}) for $^{13}C_2H_2$ resulting from the simultaneous fit of all sub-bands involving levels up to $v_4 + v_5 = 3$.[a]

Parameter		Parameter	
ω_4^0	600.0665654 (349)	y_4^{44}	−0.00610822 (552)
ω_5^0	727.1981581 (306)	y_4^{45}	0.007513 (121)
x_{44}^0	2.9964670 (229)	y_4^{55}	0.088473 (699)
x_{45}^0	−2.415569 (571)	y_5^{44}	0.060248 (182)
x_{55}^0	−2.3025686 (212)	y_5^{45}	−0.041248 (462)
y_{444}^0	0.01635771 (466)	y_5^{55}	−0.00609597 (468)
y_{555}^0	0.01301684 (453)	r_{45}^0	−6.410785 (280)
y_{455}^0	0.095427 (235)	$r_{45}^J \times 10^3$	0.1811782 (589)
y_{445}^0	−0.0275539 (625)	$r_{45}^{JJ} \times 10^9$	−3.534 (129)
g_{44}^0	0.8146064 (151)	$r_{45}^{JJJ} \times 10^{12}$	0.8951 (337)
g_{45}^0	6.649255 (568)	r_{445}	0.188728 (197)
g_{55}^0	3.4490997 (129)	r_{455}	−0.0761305 (731)
–	–	–	–
B_0	1.119574352 (174)	$\gamma^{44} \times 10^5$	−6.65551 (909)
$\alpha_4 \times 10^3$	−1.031341 (141)	$\gamma^{45} \times 10^5$	−27.3300 (496)
$\alpha_5 \times 10^3$	−1.9303064 (945)	$\gamma^{55} \times 10^5$	−9.93414 (342)
$\gamma_{44} \times 10^5$	0.29817 (455)	$\gamma_4^{44} \times 10^5$	0.10761 (288)
$\gamma_{45} \times 10^5$	4.2885 (476)	$\gamma_4^{45} \times 10^5$	0.71440 (248)
$\gamma_{55} \times 10^5$	1.77818 (458)	$\gamma_4^{55} \times 10^5$	−8.7671 (705)
$\gamma_{445} \times 10^5$	0.65795 (338)	$\gamma_5^{44} \times 10^5$	−1.12413 (718)
$\gamma_{455} \times 10^5$	2.5779 (231)	$\gamma_5^{45} \times 10^5$	5.3926 (497)
$\gamma_{555} \times 10^5$	−0.012977 (765)	$\gamma_5^{55} \times 10^5$	−0.14877 (108)
$D_0 \times 10^6$	1.487261 (172)	$\delta_{45} \times 10^9$	−0.5225 (260)
$\beta_4 \times 10^8$	2.8708 (111)	$\delta_{55} \times 10^9$	1.1362 (340)
$\beta_5 \times 10^8$	2.49530 (892)	$\delta^{45} \times 10^9$	−3.8618 (770)
$\delta_{44} \times 10^9$	−0.3788 (249)	$\delta^{55} \times 10^9$	−5.1523 (938)
$H_0 \times 10^{12}$	1.2264 (481)	$h_5 \times 10^{12}$	0.1566 (146)
$h_4 \times 10^{12}$	0.2502 (346)		
$q_4^0 \times 10^3$	4.8219495 (902)	$q_4^J \times 10^8$	−3.0132 (244)
$q_5^0 \times 10^3$	4.2352019 (568)	$q_5^J \times 10^8$	−3.35593 (595)
$q_{44} \times 10^5$	−1.58184 (279)	$q_4^{JJ} \times 10^{12}$	−2.537 (243)
$q_{45} \times 10^5$	5.4658 (242)	$q_5^{JJ} \times 10^{12}$	0.4192 (187)
$q_{54} \times 10^5$	11.01676 (346)	$q_4^{JJJ} \times 10^{15}$	0.7347 (741)
$q_{55} \times 10^5$	3.11092 (192)	$q_4^k \times 10^5$	−0.08587 (358)
		$q_5^k \times 10^5$	−1.1251 (254)
$q_{44}^{12} \times 10^5$	3.9468[b] (566)	$q_{55J}^{12} \times 10^8$	2.0609[b] (187)
$q_{55}^{12} \times 10^5$	−4.2180[b] (163)	$q_{44JJ}^{12} \times 10^{12}$	−12.711[b] (487)
$q_{44J}^{12} \times 10^8$	0.7126[b] (743)		
$\rho_4^0 \times 10^9$	−11.495 (468)	$\rho_{55} \times 10^9$	1.699 (106)
$\rho_5^0 \times 10^9$	4.037 (319)	$\rho_4^J \times 10^{12}$	2.421 (162)
$\rho_{44} \times 10^9$	1.857 (149)	$\rho_{45}^0 \times 10^9$	−6.148 (333)
$\rho_{45} \times 10^9$	−16.249 (204)	$\rho_{45}^{0J} \times 10^{12}$	−1.7426 (923)
$\rho_{54} \times 10^9$	41.582 (983)		

Number of data = 5874 Number of fitted data = 5605
Standard deviation of the fit $\times 10^4 = 1.75$

[a]Estimated errors (1σ) are given in parentheses in units of the last figure quoted.
[b]Parameter used only for the levels of the manifold ($v_4 = 1$, $v_5 = 2$).

Table 3. Spectroscopic parameters (in cm^{-1}) for $^{13}C_2H_2$ resulting from the separate fits of all sub-bands involving levels of the manifolds with $v_4 + v_5 = 4$.[a]

$v_4 = 1,\ v_5 = 3$		$v_4 = 3,\ v_5 = 1$	
Parameter		Parameter	
y^0_{4555}	0.01899505 (220)	$y^0_{4445} \times 10^3$	−1.48437 (280)
y^{55}_{45}	−0.04286187 (488)	$y^{45}_{44} \times 10^3$	−0.03335 (424)
$r_{4555} \times 10^3$	−2.96000 (159)	$r_{4445} \times 10^3$	0.78146 (137)
$r^J_{455} \times 10^6$	5.7894 (718)	$r^J_{445} \times 10^6$	−4.2932 (330)
$\gamma_{4555} \times 10^3$	−0.0121976 (239)	$\gamma_{4445} \times 10^6$	−1.9016 (226)
$y^{55}_{45} \times 10^3$	0.0292620 (431)	$y^{45}_{44} \times 10^6$	−4.3538 (382)
$\delta_{455} \times 10^9$	−0.5924 (383)	$\delta_{445} \times 10^9$	−3.251 (106)
$q_{444} \times 10^3$	0.05997 (287)	$\delta^{45}_4 \times 10^9$	−4.161 (164)
$q_{555} \times 10^3$	−0.0045673 (833)	$q_{444} \times 10^6$	−0.8230 (187)
$\rho^0_{455} \times 10^6$	−0.059318 (464)	$q^J_{44} \times 10^9$	−2.2054 (805)
Number of data = 900		Number of data = 884	
Number of fitted data = 809		Number of fitted data = 800	
Standard deviation of the fit $\times 10^4 = 3.8$		Standard deviation of the fit $\times 10^4 = 3.5$	
$v_4 = 0,\ v_5 = 4$		$v_4 = 2,\ v_5 = 2$	
Parameter		Parameter	
$y^0_{5555} \times 10^3$	0.023253 (157)	y^0_{4455}	0.0475624 (182)
$y^{55}_{55} \times 10^3$	−0.015141 (356)	$y^{44}_{45} \times 10^3$	0.4351 (141)
$\gamma_{5555} \times 10^6$	0.02130 (116)	y^{45}_{45}	0.0236029 (186)
$y^{55}_{55} \times 10^6$	−0.04537 (266)	y^{55}_{45}	−0.0732581 (302)
$\delta_{555} \times 10^9$	−0.52248 (666)	r_{4455}	1.35099810 (442)
$\delta^{55}_5 \times 10^9$	1.0730 (149)	$r^J_{445} \times 10^3$	−0.104710 (153)
$q_{555} \times 10^6$	3.5946 (296)	$\gamma_{4455} \times 10^6$	−8.796 (221)
$q^J_{55} \times 10^9$	−5.886 (355)	$\gamma^{44}_{44} \times 10^6$	−5.494 (169)
$q^{JJ}_{55} \times 10^{12}$	3.401 (254)	$\gamma^{45}_{45} \times 10^6$	−40.019 (218)
$\rho^J_{55} \times 10^{12}$	−1.6295 (377)	$\gamma^{55}_{44} \times 10^6$	6.620 (361)
		$\delta_{445} \times 10^6$	0.05654 (189)
		$\delta^{44}_4 \times 10^6$	−0.03289 (107)
		$\delta^{55}_5 \times 10^6$	−0.05999 (217)
		$q_{444} \times 10^3$	−2.426477 (907)
		$q_{555} \times 10^3$	0.028593 (966)
		$q^J_{44} \times 10^6$	0.024077 (951)
		$\rho_{444} \times 10^6$	0.21374 (344)
		$\rho_{555} \times 10^6$	0.20497 (531)
		$\rho^J_{44} \times 10^9$	−0.06560 (390)
		$\rho^J_{55} \times 10^9$	0.08797 (888)
		$\rho^0_{445} \times 10^6$	0.32547(494)
Number of data = 606		Number of data = 1265	
Number of fitted data = 576		Number of fitted data = 1089	
Standard deviation of the fit $\times 10^4 = 3.5$		Standard deviation of the fit $\times 10^4 = 4.4$	

[a]Estimated errors (1σ) are given in parentheses in units of the last figure quoted.
The parameters in Table 2 have been constrained in the analysis.

The measured wavenumbers of the transitions, together with their quantum number assignments, the corresponding (observed–calculated) values obtained with the parameters in Tables 2 and 3, and the energies of the levels involved in the transitions, available as supplementary material, can be obtained from the Bologna authors.

5. Conclusions

The infrared absorption spectrum of ^{13}C substituted acetylene, $^{13}C_2H_2$, was recorded at high resolution between 60 and 2800 cm^{-1}. Analysis of the various observed bands confirmed the previous results [6,13] and extended the assignments to excited bending levels

Table 4. Term values (in cm^{-1}) of the various observed l-sublevels in $^{13}C_2H_2$.[a]

v_4	v_5	Symmetry	l_4	l_5	Value[b]
1	0	Π_g	±1	0	602.7673
0	1	Π_u	0	±1	727.2302
2	0	Δ_g	±2	0	1210.9738
2	0	Σ_g^+	0	0	1212.2499
1	1	Σ_u^+	1	−1	1317.2394
1	1	Σ_u^-	−1	1	1329.6106
1	1	Δ_u	±1	±1	1332.1674
0	2	Σ_g^+	0	0	1445.2902
0	2	Δ_g	0	±2	1454.5454
3	0	Φ_g	±3	0	1824.6768
3	0	Π_g	±1	0	1827.2833
2	1	$^{II}\Pi_u$	0	±1	1920.2131
2	1	$^{I}\Pi_u$	±2	*1	1939.8001
2	1	Φ_u	±2	±1	1942.6195
1	2	$^{II}\Pi_g$	±1	0	2035.2778
1	2	$^{I}\Pi_g$	*1	±2	2053.0143
1	2	Φ_g	±1	±2	2061.9318
0	3	Π_u	0	±1	2163.5282
0	3	Φ_u	0	±3	2181.9787
3	1	$^{II}\Delta_u$	±3	*1	2528.0797
3	1	Σ_u^+	1	−1	2531.6131
3	1	Σ_u^-	−1	1	2554.7956
2	2	$^{II}\Sigma_g^+$	2	−2	2626.4331
2	2	Σ_g^-	−2	2	2639.4587
2	2	$^{II}\Delta_g$	±2	0	2640.0901
2	2	$^{I}\Sigma_g^+$	0	0	2662.2073
2	2	$^{I}\Delta_g$	0	±2	2666.2539
1	3	Σ_u^+	−1	1	2743.4210
1	3	$^{II}\Delta_u$	±1	±1	2754.1791
1	3	Σ_u^-	1	−1	2768.9619
0	4	Σ_g^+	0	0	2872.7906
0	4	Δ_g	0	±2	2881.9798
0	4	Γ_g	0	±4	2909.5677

[a]Upper signs of l_4 or l_5 refer to 'e' states; lower signs refer to 'f' states.
[b]Term values areρ_{44} expressed as $G_v^0 - B_v k^2 - D_v k^4$.

up to $v_{tot} = 4$. A total of 9529 transitions belonging to 101 bands were identified and analyzed allowing the characterization of the ground state and of 33 vibrationally excited states. A simultaneous fit of all the assigned transitions involving states up to $v_{tot} = 3$ was carried out on the basis of a model Hamiltonian containing, in addition to the usual rotation–vibration parameters, the l-type resonance constants. A set of 80 statistically significant molecular parameters were obtained from the analysis of the levels up to $v_{tot} = 3$. The energies of the levels of the $v_{tot} = 4$ manifolds are affected by various kind of perturbations which prevented the determination of an appropriate set of parameters. Four sets of effective parameters reproduced the observed transition wavenumbers with a standard deviation larger than that obtained for $v_{tot} = 3$. Altogether, out of 9529 assigned transition wavenumbers 8877 were retained in the final fits.

Acknowledgements

The authors wish to thank Canadian Light Source, which is supported by NSERC, NRC, CIHR and the University of Saskatchewan, where the FIR spectra were recorded, and Dr J.W.C. Johns (NRCC Ottawa) for the recording of the spectra in the 700 cm^{-1} region. G.D.L. and L.F. acknowledge the financial support of the Ministero dell'Istruzione dell'Università e della Ricerca (PRIN "Spettroscopia molecolare per la Ricerca Atmosferica e Astrochimica: Esperimento, Teoria ed Applicazioni"). M.H. thanks the Action de Recherches Concertées de la Communauté française de Belgique for financial support.

References

[1] W.J. Lafferty and R.J. Thibault, J. Mol. Spectrosc. **14**, 79 (1964).
[2] S. Ghersetti, A. Baldacci, S. Giorgianni, R.H. Barnes and K. Narahari Rao, Gazz. Chim. It. **105**, 875 (1975).
[3] S.P. Reddy, V.M. Devi, A. Baldacci, W. Ivancic and K. Narahari Rao, J. Mol. Spectrosc. **74**, 217 (1979).
[4] P.P. Das, V.M. Devi and K. Narahari Rao, J. Mol. Spectrosc. **84**, 313 (1980).
[5] J. Hietanen, V.M. Horneman, R. Anttila and J. Kauppinen, Mol. Phys. **59**, 587 (1986).
[6] G. Di Lonardo, P. Ferracuti, L. Fusina, E. Venuti and J.W.C. Johns, J. Mol. Spectrosc. **161**, 466 (1993).
[7] G. Di Lonardo, P. Ferracuti, L. Fusina and E. Venuti, J. Mol. Spectrosc. **164**, 219 (1994).
[8] E. Venuti, G. Di Lonardo, P. Ferracuti, L. Fusina and I.M. Mills, Chem. Phys. **190**, 279 (1995).
[9] F. Alboni, G. Di Lonardo, P. Ferracuti, L. Fusina, E. Venuti and K.A. Mohamed, J. Mol. Spectrosc. **169**, 148 (1995).
[10] M. Becucci, E. Castellucci, L. Fusina and H.W. Schrötter, J. Raman Spectrosc. **29**, 237 (1998).
[11] D. Bermejo, P. Cancio, G. Di Lonardo and L. Fusina, J. Chem. Phys. **108**, 7224 (1998).
[12] D. Bermejo, R.Z. Martinez, G. Di Lonardo and L. Fusina, J. Chem. Phys. **111**, 519 (1999).
[13] G. Di Lonardo, L. Fusina, E. Venuti, J.W.C. Johns, M.I. El Idrissi, J. Liévin and M. Herman, J. Chem. Phys. **111**, 1008 (1999).
[14] J.W.C. Johns, J. Opt. Soc. Am. **B2**, 1340 (1985).
[15] F. Matsushima, H. Odashima, T. Iwasaki, S. Tsunekawa and K. Takagi, J. Mol. Struct. **352/353**, 371 (1995).
[16] G. Guelachvili and K. Narahari Rao, *Handbook of Infrared Standards* (Academic Press, San Diego, 1986).
[17] J.W.C.Johns, 45th Ohio State University Symposium on Molecular Spectroscopy, paper TB7, 1990.
[18] A.G. Maki and J.S. Wells, *Wavenumber Calibration Tables From Heterodyne Frequency Measurements*.

NIST Special Publication 821, U.S. Government Printing Office, Washington, 1991.
[19] R.A. Toth, J. Opt. Soc. Am. **B8**, 2236, ibid., **B10**, 2006 (1993) (1991).
[20] G. Guelachvili and K. Narahari Rao, *Handbook of Infrared Standards* (Academic Press, San Diego, 1986).
[21] G. Guelachvili and 23 other authors, Pure Appl. Chem. **68**, 193 (1996).
[22] B. Amyay, M. Herman, A. Fayt, L. Fusina and A. Predoi-Cross, Chem. Phys. Lett. **491**, 17 (2010).
[23] Y. Kabbadj, M. Herman, G. Di Lonardo, L. Fusina and J.W.C. Johns, J. Mol. Spectrosc. **150**, 535 (1991).
[24] T.R. Huet, M. Herman and J.W.C. Johns, J. Chem. Phys. **94**, 3407 (1991).
[25] S. Robert, M. Herman, J. Vander Auwera, G. Di Lonardo, L. Fusina, G. Blanquet, M. Lepere and A. Fayt, Mol. Phys. **105**, 587 (2007).
[26] G. Di Lonardo, A. Baldan, G. Bramati and L. Fusina, J. Mol. Spectrosc. **213**, 57 (2002).